Stem Cell Reports
Resource
OPEN ACCESS

Long-Term Expandable SOX9^{+} Chondrogenic Ectomesenchymal Cells from Human Pluripotent Stem Cells

Katsutsugu Umeda,[1,3] Hirotsugu Oda,[2] Qing Yan,[1,4] Nadine Matthias,[1] Jiangang Zhao,[1,5] Brian R. Davis,[1] and Naoki Nakayama[1,*]

[1]Institute of Molecular Medicine, The University of Texas Health Science Center at Houston Medical School, Houston, TX 77030, USA
[2]Department of Pediatrics, Kyoto University School of Medicine, Kyoto 606-8507, Japan
[3]Present address: Department of Pediatrics, Kyoto University School of Medicine, Kyoto 606-8507, Japan
[4]Present address: Houston Methodist Research Institute, Houston, TX 77030, USA
[5]Present address: The University of Texas Medical Branch at Galveston, Galveston, TX 77555, USA
*Correspondence: naoki.nakayama@uth.tmc.edu
http://dx.doi.org/10.1016/j.stemcr.2015.02.012

SUMMARY

Here we report the successful generation and long-term expansion of SOX9-expressing CD271^{+}PDGFRα^{+}CD73^{+} chondrogenic ectomesenchymal cells from the *PAX3/SOX10/FOXD3*-expressing MIXL1^{-}CD271^{hi}PDGFRα^{lo}CD73^{-} neural crest-like progeny of human pluripotent stem cells in a chemically defined medium supplemented with Nodal/Activin/transforming growth factorβ (TGFβ) inhibitor and fibroblast growth factor (FGF). When "primed" with TGFβ, such cells efficiently formed translucent cartilage particles, which were completely mineralized in 12 weeks in immunocompromized mice. The ectomesenchymal cells were expandable without loss of chondrogenic potential for at least 16 passages. They maintained normal karyotype for at least 10 passages and expressed genes representing embryonic progenitors (*SOX4/12, LIN28A/B*), cranial mesenchyme (*ALX1/3/4*), and chondroprogenitors (*SOX9, COL2A1*) of neural crest origin (*SOX8/9, NGFR, NES*). Ectomesenchyme is a source of many craniofacial bone and cartilage structures. The method we describe for obtaining a large quantity of human ectomesenchymal cells will help to model craniofacial disorders in vitro and potentially provide cells for the repair of craniofacial damage.

INTRODUCTION

Adult mesenchymal stromal cells (MSCs), defined in vitro by their potential to contribute to bone-cartilage-fat cell lineages, are currently used for cell-based bone and cartilage therapies because of their ready accessibility. However, as for other adult stem cells, it is difficult to obtain sufficient MSCs for treatment. Expansion culture is therefore necessary before transplantation; however, it tends to cause the loss of long-term viability of the MSCs and their capacity to differentiate, especially into chondrocytes (Somoza et al., 2014). Different types of bone and cartilage are formed most actively during embryonic skeletogenesis from one of three precursor cell types: paraxial mesoderm, lateral plate mesoderm, and cranial neural crest. Such embryonic cells and their osteochondrogenic progeny may be as effective as or more effective than MSCs for the regeneration of adult bone and cartilage.

The early processes of in vitro differentiation of pluripotent embryonic stem cells (ESCs) mimic those of in vivo embryogenesis (Nishikawa et al., 2007). Therefore, ESCs and induced pluripotent stem cells (iPSCs) (collectively designated pluripotent stem cells or PSCs) would appear to be the practical source of embryonic precursor cells in humans. In fact, in vitro induction of osteogenesis and chondrogenesis from human PSCs (hPSCs) and mouse (mPSCs) has been demonstrated by many groups (Nakayama and Umeda, 2011). With the exception of recent reports, including ours (Craft et al., 2013; Diekman et al., 2012; Nakayama et al., 2003; Toh et al., 2009; Umeda et al., 2012; Zhao et al., 2014), many of the earlier reports described spontaneous differentiation of hPSCs followed by enrichment of mesenchymal cells by further culturing the progeny in MSC medium. As adult human tissue-derived MSCs or chondroprogenitors (Koelling et al., 2009; Pittenger et al., 1999), mesenchymal cells derived from mESCs/iPSCs were able to be expanded extensively; however, expansion occurred with the loss of their chondrogenic activity (Bakre et al., 2007; Diekman et al., 2012). Thus far, the potential benefits of bone and cartilage repair of hPSC-derived osteochondroprogenitors over those of adult MSCs, whether in quantity or in quality, have not been demonstrated, even in vitro (Nakayama and Umeda, 2011). In theory, the wealth of information on the signaling mechanisms involved in mouse skeletogenesis should be of great help in improving the expansion culture methods. However, the unclear embryonic origins of the chondrogenic activity developed from PSCs and the undefined conditions used for expansion have hampered full use of the information and thereby hindered progress.

A large portion of craniofacial bone and cartilage arises from osteochondrogenic progeny (i.e., ectomesenchyme) from cranial neural crest (Santagati and Rijli, 2003), generated from the junction between anterior neuroectoderm

and surface ectoderm (Milet and Monsoro-Burq, 2012). Neural crest cells have been developed from hESCs in 12–28 days of differentiation culture either through neuroepithelial intermediates induced by suppression of Nodal/Activin/transforming growth factor β (TGFβ) and bone morphogenetic protein (BMP) signaling in a defined medium (Chambers et al., 2009; Smith et al., 2008) or directly by activation of WNT signaling with suppression of Nodal/Activin/TGFβ signaling (Menendez et al., 2011). Further differentiation and expansion for 2–3 weeks of such neural crest cells or earlier neural cells in a serum-containing medium generate MSC-like cells with variable chondrogenic activity, but never sufficient to reproducibly form cartilage particles that accumulate proteoglycan-rich, mature matrices uniformly (hereafter designated "full-cartilage").

Our group has focused on generating and characterizing paraxial mesodermal progeny from mPSCs/hPSCs, which are highly chondrogenic (Tanaka et al., 2009; Umeda et al., 2012; Zhao et al., 2014). In the current study, we report simple, effective methods for the specification of neural crest-like progeny from hPSCs and subsequent generation and expansion of chondrogenically committed ectomesenchymal cells without loss of their chondrogenic activity over 7–8 weeks in chemically defined media (CDM). The outcomes were achieved by the control of fibroblast growth factor (FGF) signaling and Nodal/Activin/TGFβ signaling. We have also defined the cellular developmental pathway from hPSCs to such ectomesenchymal cells using the neural crest markers the low-affinity nerve growth factor receptor (CD271) (Lee et al., 2007; Stemple and Anderson, 1992), and the platelet-derived growth factor receptor α (PDGFRα) (Morrison-Graham et al., 1992; Weston et al., 2004), and the MSC markers, CD73 and CD13 (Olivier et al., 2006; Pittenger et al., 1999).

RESULTS

Signaling Requirement for Early Development of Neural Crest-like Progeny from hPSCs

Generation of osteochondrogenic ectomesenchyme from hPSCs first requires specification of cranial neural crest-like progeny. In order to reproducibly generate strong chondrogenic activity from hPSCs, we first optimized the method for specification of neural crest using CD271 as the readout. Fluorescence-activated cell sorting (FACS) analyses revealed that when H9 hESCs and BJ5 hiPSCs were differentiated in CDM using the conventional embryoid body (EB)-forming culture or 2D differentiation culture in the presence of SB431542 or other Nodal/Activin/TGFβ signaling inhibitor (e.g., A83-01 or SJN2511), they generated progeny that expressed CD271 (Figures 1A and S1). The $CD271^{hi}$ cell population, but not the $CD271^{lo/-}$ progeny, also expressed PDGFRα at low levels. Both populations lacked CD73 and CD13. The effect of SB431542 was dose dependent at least up to 10 μM (Figure S1D).

The $CD271^{hi}PDGFR\alpha^{lo}$ cell development reached a peak around day 6 of differentiation (Figure S1C), in parallel with the highest expression of the "neural crest specifier" genes *PAX3* and *PAX7* (Nelms and Labosky, 2010) (Figure 1B). In contrast, the neuroectoderm marker *SOX1* was never induced, and the ESC marker *NANOG* was downregulated. Furthermore, the isolated $CD271^{hi}(PDGFR\alpha^{lo})CD73^{-}$ progeny had higher levels of *SOX10* and *FOXD3* transcripts than the $CD271^{lo/-}(PDGFR\alpha^{-})CD73^{-}$ cells, indicating enrichment of the fraction with neural crest-like progeny (Figure 1D). SOX9 is also implicated in the specification of cranial neural crest (Nelms and Labosky, 2010) and is expressed in premigratory human neural crest (Betters et al., 2010). The SOX9 reporter, GFP (Figures 1F and S1I) and *SOX9* transcripts (Figure S1G) were expressed in the $CD271^{hi}CD73^{-}$ fraction. The PAX3 protein (Figure 1E) and *PAX3* transcript (Figure S1G) were also detected in the $CD271^{hi}CD73^{-}$ fraction.

Furthermore, in sharp contrast to the results obtained from the hPSC differentiation to paraxial mesoderm (Umeda et al., 2012), when *MIXL1* (an early mesendoderm gene)-green fluorescence protein (GFP) knockin hESCs (MIXL1-GFP) (Davis et al., 2008) were differentiated under similar conditions, no $MIXL1\text{-}GFP^{+}$ progeny developed (Figure 1A). There was also negligible induction of a second mesendoderm transcript, *T* (Figure S1B) (Umeda et al., 2012). Therefore, neither $CD271^{hi}(PDGFR\alpha^{lo})CD73^{-}$ nor $CD271^{lo}(PDGFR\alpha^{-})CD73^{-}$ cells were likely to be mesendodermal derivatives.

BMP and WNT are implicated in the neural crest specification (Milet and Monsoro-Burq, 2012). As expected, the BMP inhibitor Noggin suppressed the SB431542-induced development of the $CD271^{hi}PDGFR\alpha^{lo}(CD73^{-})$ neural crest-like progeny from H9 hESCs (Figure S1E). The WNT inhibitor FZD also showed an inhibitory effect, consistent with the findings of Menendez et al. (2011) (Figure S1D). Interestingly, BMP4 at 10 ng/ml, a concentration sufficient to induce mesoderm (Wang and Nakayama, 2009), was as inhibitory as Noggin, and the GSK3 inhibitor that mimics canonical WNT signaling showed weakly inhibitory effects (Figure S1E). However, when SOX9-GFP iPSCs were used, the GSK3 inhibitor was found to enhance the genesis of $CD271^{hi}CD73^{-}$ cells (Figure S1I).

Thus, inhibition of Nodal/Activin/TGFβ signaling with appropriate levels of BMP and WNT signaling is required for the effective development of $CD271^{hi}PDGFR\alpha^{lo}CD73^{-}CD13^{-}$ neural crest-like progeny from hPSCs (hereafter called $CD271^{hi}CD73^{-}$ progeny) more quickly than previously attained (Lee et al., 2010; Menendez et al., 2011), potentially reflecting the specification of cranial instead of trunk neural crest cells.

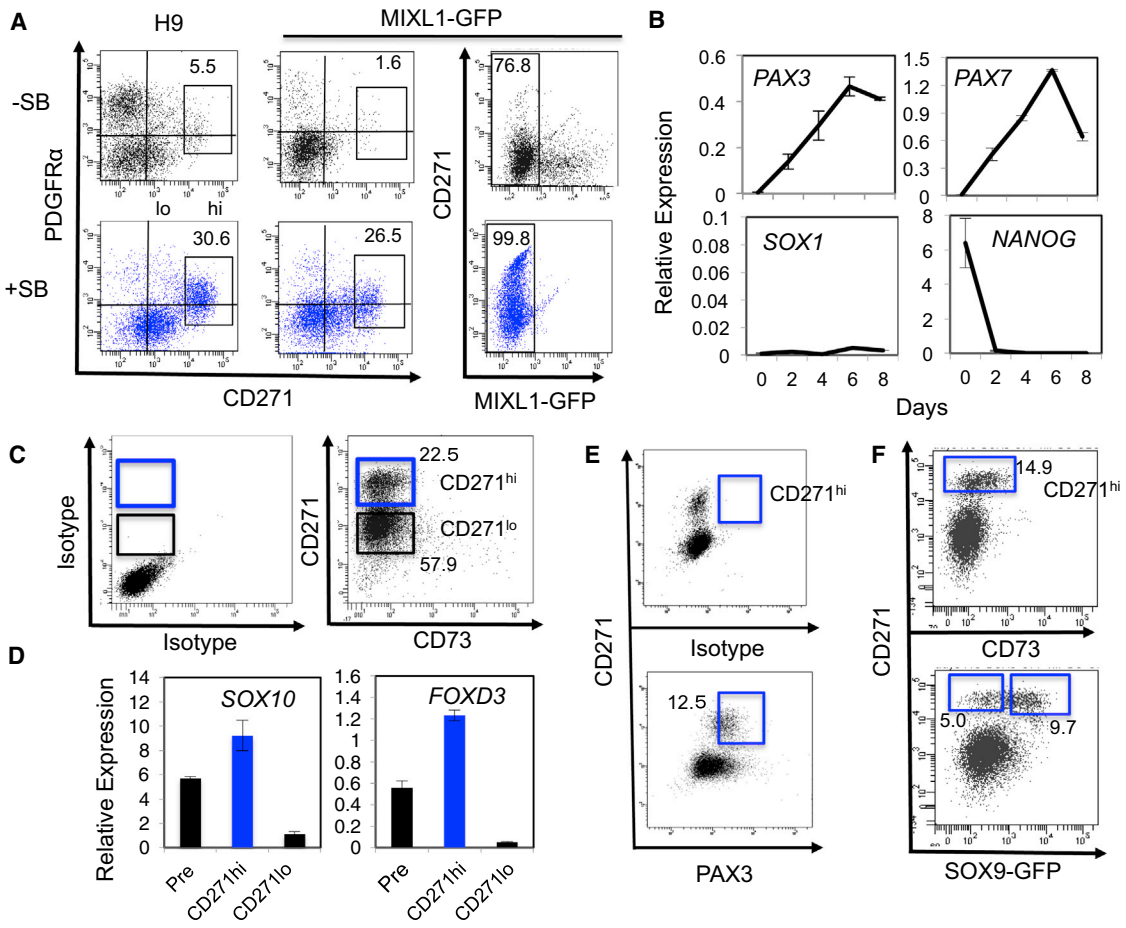

Figure 1. Directed Specification of Neural Crest from hPSCs

(A) FACS analysis demonstrating the SB431542-dependent development of $CD271^{hi}PDGFR\alpha^{lo}$ progeny during 2D differentiation of H9 and MIXL1-GFP hESCs in CDM. SB: 10 μM SB431542.

(B) Time-dependent changes in the gene expression profile during differentiation of H9 hESCs in the presence of SB (n = 3 technical repeats, mean ± SD).

(C) Isolation of H9-derived $CD271^{hi}(PDGFR\alpha^{lo}CD73^{-})$ and $CD271^{lo}(PDGFR\alpha^{-}CD73^{-})$ progeny by FACS. (Left) Isotype control.

(D) Real-time RT-PCR analysis with cells from (C) demonstrating enrichment of neural crest-related transcripts in the $CD271^{hi}CD73^{-}$ cell fraction. Pre, presort cells (n = 3 technical repeats, mean ± SD).

(E) Intracellular FACS staining by anti-PAX3 antibody demonstrating presence of PAX3 protein in the H9-derived $CD271^{hi}CD73^{-}$ cell fraction. (Upper) Isotype control.

(F) FACS demonstration of SOX9-GFP expression in the $CD271^{hi}CD73^{-}$ progeny in SOX9-GFP hiPSCs differentiated for 6 days.

Mesenchymal Cells Derived from the Nonmesendodermal hESC Progeny by Conventional Methods Show Weak, Transient Chondrogenic Activity

The neural crest-like progeny were then directed to commit to chondrogenic ectomesenchyme. First, using a conventional EB-outgrowth method (Hwang et al., 2006) (Figure S2A), we generated mesenchymal cells from the SB431542-treated H9 and MIXL1-GFP hESCs. In knockout serum replacement-based SR medium or serum-containing D10 medium, expansion of the outgrowth cells led to enhanced expression of CD73 and later CD13, but loss of the expression of CD271 (Figures S2D and S2E). As we reported previously (Umeda et al., 2012), $MIXL1\text{-}GFP^{+}$ mesendodermal progeny were never detected during such studies (data not shown).

In 3D-pellet culture, the generated mesenchymal cells gave rise to a particle containing an area that weakly stained metachromatically (pink to purple) with Toluidine Blue and immunostained with anti-type II collagen (COL2) antibody at passage 1 (p1) (Figure S2F) and p2, but not from p3 to p5. The lack of chondrogenic activity in the primary

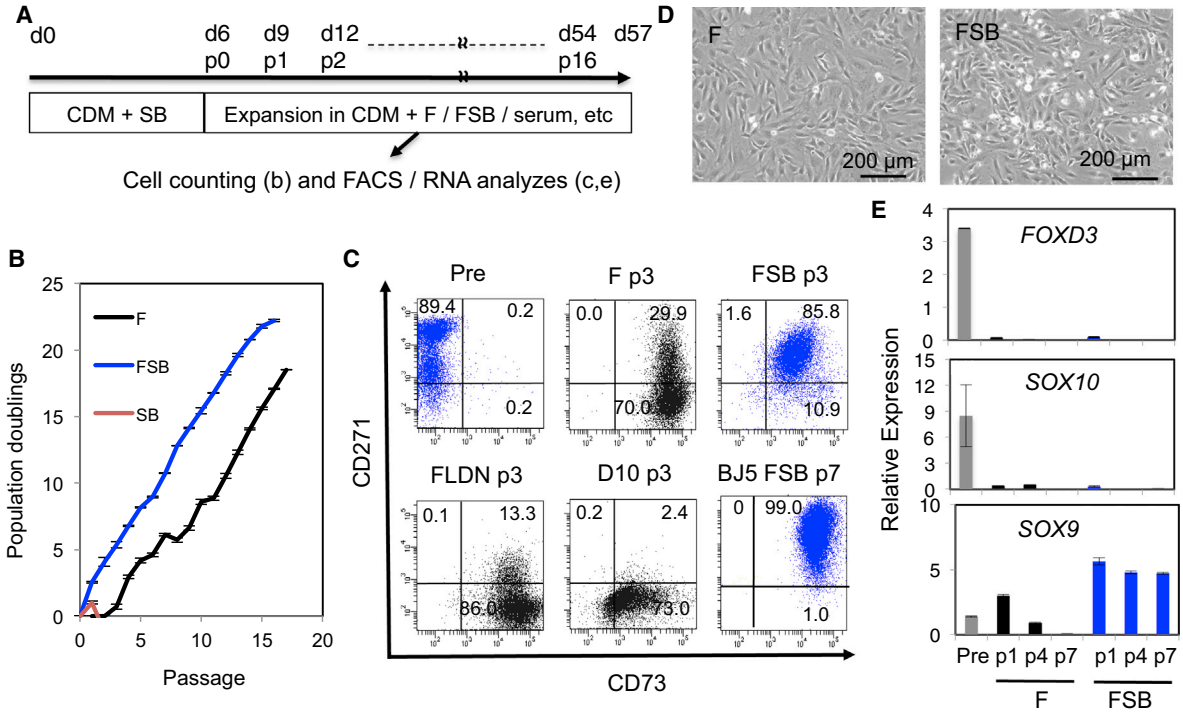

Figure 2. FGF2+SB431542 Generates and Expands *SOX9*-Expressing CD271$^+$PDGFRα$^+$CD73$^+$ Ectomesenchymal Cells from Unsorted Nonmesendodermal Progeny

(A) Graphical representation of the experimental procedure. SB, SB431542; F, FGF2; FSB, FGF2+SB431542.

(B) Growth curve of H9 hESC-derived ectomesenchymal cells expanded under F, FSB, and SB conditions (n = 3 independent cultures, mean ± SD).

(C) FACS analysis demonstrating the effect of FSB on the selective accumulation of CD271$^+$CD73$^+$ mesenchymal. H9 hESCs and BJ5 hiPSCs were differentiated (Pre) and expanded under the conditions indicated: D10, F, FSB, and FLDN (FGF2+LDN193189). p, passage; isotype control, Figure S3C.

(D) Micrographs of mesenchymal cells (p4) expanded under F and FSB.

(E) Real-time RT-PCR analysis demonstrating changes in the neural crest gene expression during expansion under F and FSB (n = 3 technical repeats, mean ± SD).

outgrowth cells (p0), suggests that a short-term expansion of the outgrowth cells is required for its development and/or accumulation. However, as reported by others (Nakayama and Umeda, 2011), we did not observe robust chondrogenic activity leading to a full-cartilage particle, as found for paraxial mesoderm derived from mPSCs and hPSCs (Nakayama et al., 2003; Umeda et al., 2012). Thus, conventional culture methods failed to generate and maintain strong chondrogenic activity from hPSC-derived neural crest-like progeny.

Generation and Selective Expansion of CD271$^+$PDGFRα$^+$CD73$^+$ Mesenchymal Cells in CDM in the Presence of FGF2 and SB431542

Either in a FACS-purified form or in an unpurified mixture with other nonmesendodermal (i.e., MIXL1$^-$) cells, the CD271^{hi}CD73$^-$ neural crest-like progeny failed to adhere to the culture dish in the absence of fibronectin and grew poorly in the medium in which they were specified, i.e., CDM plus SB431542 (SB; Figures 2B and S3A). Therefore, we tested the effects of growth factors, such as FGF2 that have been used for maintaining neural crest cells (Stemple and Anderson, 1992) and generating chondrogenic activity (Abzhanov et al., 2003) in culture, and of other factors, such as endothelin1, PDGF, and Sonic hedgehog that have been linked to cranial skeletogenesis and ectomesenchymal specification in vivo (Le Douarin and Creuzet, 2009). FGF2 alone significantly increased viability and supported growth of the neural crest-like progeny on fibronectin but was often associated with significant slowdown in an early stage of expansion culture. The addition of both FGF2 and SB431542 maintained the growth rate at least until p16 and supported maintenance of the normal karyotype at least to p10 (Figure S3B).

Direct expansion of the nonmesendodermal progeny mix in CDM in the presence of FGF2 and SB431542

resulted in accumulation of CD271$^+$PDGFRα$^+$CD73$^+$ mesenchymal cells (Figures 2C, S3, and S4). The cells were positive for the MSC markers CD105, CD166, CD29, CD44, and CD56, but negative for MSC markers CD13 and STRO1 (Figures S3D and S3E). In contrast, CD271 expression decreased in the presence of FGF2 alone, causing the CD271$^-$PDGFRα$^+$CD73$^+$ cells to become the predominant cell population by p3 (Figure 2C). Similar results were obtained from expansion in D10 medium. The BMP receptor inhibitor LDN193189 was unable to replace SB431542. Interestingly, as with EB-outgrowth cell culture (Figures S2D and S2E), CD13$^+$ cells appeared later (from p6) under FGF2, but not FGF2+SB431542, conditions (Figure S3D).

The expression of the neural crest genes *FOXD3* and *SOX10* was quickly downregulated during expansion under either FGF2 or FGF2+SB431542 conditions, even at p1, indicating rapid non-neural commitment of the neural crest-like progeny (Figure 2E) (Nelms and Labosky, 2010). In contrast, the *SOX9* transcript was strongly upregulated at p1 and maintained over seven passages under FGF2+SB431542 conditions, whereas the *SOX9* transcript was slightly enhanced at p1 and gradually declined after p4 under FGF2 conditions.

Our results indicate that activation of FGF signaling and suppression of Nodal/Activin/TGFβ signaling during expansion of the unsorted nonmesendodermal progeny of hPSCs selectively lead to the accumulation of *SOX9*-expressing CD271$^+$PDGFRα$^+$CD73$^+$CD13$^-$ ectomesenchymal cells (hereafter called CD271$^+$CD73$^+$ cells).

The CD271$^+$CD73$^+$ Ectomesenchymal Cells Are Derived from the CD271^{hi}CD73$^-$ Neural Crest-like Progeny

To determine the cellular origin of the CD271$^+$CD73$^+$ ectomesenchymal cells expanded under FGF2+SB431542 conditions, the CD271^{hi}CD73$^-$ and CD271^{lo}CD73$^-$ progeny, developed from H9 hESCs and BJ5 hiPSCs, were sorted by FACS (Figures 1C and S1H) and then cultured in CDM in the presence of FGF2 and one of three Nodal/Activin/TGFβ inhibitors, SB431542, A83-01, or SJN2511. While FGF2 alone supported the accumulation of CD271$^-$CD73$^+$ cells from either progeny, the FGF2+SB431542, FGF2+A83-01, and FGF2+SJN2511 conditions preferentially supported the development of CD271$^+$CD73$^+$ cells from the sorted CD271^{hi}CD73$^-$ neural crest-like progeny (Figures 3B and S4G). Concentrations of SB431542 between 1 and 3 μM were sufficient for the stable maintenance of CD271$^+$CD73$^+$ cells (Figure S3C). On the other hand, most of the CD271^{lo}CD73$^-$ progeny did not survive, even under FGF2+SB431542 conditions, and the derived mesenchymal cells were a mixture of CD271$^+$CD73$^+$ and CD271$^-$CD73$^+$ cells (Figures 3B and S4G) from which the CD271$^+$CD73$^+$ cells were later lost.

Even at the early p3 stage, *SOX9* expression was clearly observed in the (FGF2+SB431542)-cultured, but not the FGF2-cultured CD271^{hi}CD73$^-$ neural crest-like cells (Figure 3C). *SOX9* expression was not sustained during the growth of CD271^{lo}CD73$^-$ cells under either condition. The nuclear localization of SOX9 protein was also obvious in 76% (p10) to 85% (p8) of the (FGF2+SB431542)-expanded CD271$^+$CD73$^+$ cells, of which approximately 20% displayed strong signals (Figure 3D). In support of this finding, expansion of SOX9-GFP hiPSC-derived CD271^{hi}CD73$^-$ neural crest-like cells under FGF2+SB431542 for five passages demonstrated that approximately 20% of the cells remained CD271$^+$GFP$^+$, while the rest became CD271$^+$GFP^{lo}. No cells became CD271$^+$GFP$^-$ (Figure 3E).

Our results indicate that SOX9-positive CD271$^+$CD73$^+$ ectomesenchymal cells were generated and then expanded from the CD271^{hi}CD73$^-$ neural crest-like progeny of hPSCs in CDM in the presence of FGF2 and Nodal/Activin/TGFβ inhibitors and that changes to this growth condition led to the generation of *SOX9*-negative CD271$^-$CD73$^+$ mesenchymal cells.

The CD271$^+$CD73$^+$ Cells Maintain Measurable Chondrogenic Activity during Expansion

Since the CD271$^+$CD73$^+$ ectomesenchymal cells maintained in FGF2+SB431542 express SOX9, we sought to demonstrate that they were chondrogenic using 2D micromass culture. Under the condition in which PDGF-BB was added to the chondrogenesis medium on day 0 and then replaced with TGFβ3 on day 6, which was supplemented with BMP4 on day 10 (hereafter designated as PDGF/TGFβ/BMP condition) (Umeda et al., 2012), CD271$^+$CD73$^+$ cells gave rise to acid Alcian Blue-positive cartilage nodules, the capacity of which lasted at least until p10 (i.e., 5 weeks) of expansion culture (Figures 3F and S4A). In contrast, the CD271$^-$CD73$^+$ cells generated and maintained under FGF2 conditions showed weak chondrogenic activity as early as p3. The SB431542-cultured cells showed no chondrogenic activity and ceased to grow at p2.

Brief Treatment with TGFβ Facilitates Formation of Macroscopic Cartilage Particle Formation from the CD271$^+$CD73$^+$ Cells

The ectomesenchymal cells expanded in CDM in the presence of FGF2 or FGF2+SB431542 were subjected to 3D-pellet culture under the PDGF/TGFβ/BMP condition. The early (p2) FGF2-expanded cells formed a large cartilage particle that stained metachromatically (pink to purple) with Toluidine Blue, but then lost such chondrogenic activity by

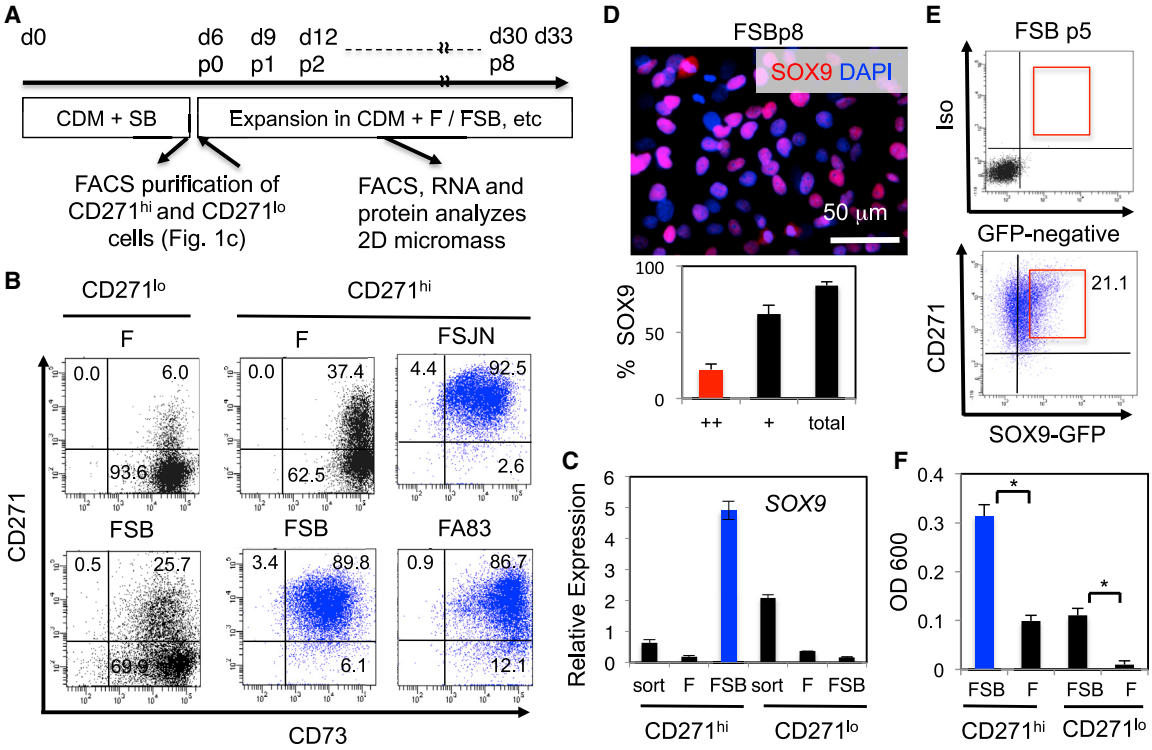

Figure 3. The SOX9-Expressing CD271^{+}CD73^{+} Ectomesenchymal Cells Are Chondrogenic and Derived from the CD271^{hi}CD73^{-} Neural Crest-like Cell Fraction

(A) Graphical representation of the experimental procedure.

(B) FACS analysis of the sorted CD271^{hi}CD73^{-} (CD271^{hi}) and CD271^{lo}CD73^{-} (CD271^{lo}) progeny, expanded under F, FSB, FSJN (FGF2+SJN2511), and FA83 (FGF2+A83-01) for three passages.

(C) Real-time RT-PCR with cells in (B) demonstrating *SOX9* expression specifically maintained in the FSB-expanded CD271^{hi} cells. sort, pre-expanded cells (n = 3 technical repeats, mean ± SD).

(D) Immunofluorescence detection of SOX9 protein in the FSB-expanded CD271^{hi} cells. Pink, SOX9; blue (nucleus), DAPI; graph, the value of % SOX9^{+} nuclei was the average of scoring from four areas (n = 4 technical repeats, mean ± SD); ++, strong signal; +, weaker signal; isotype control, Figure S4J.

(E) SOX9-GFP expression in the FSB-expanded CD271^{hi} cells. SOX9-GFP hiPSCs were differentiated, and the CD271^{hi}CD73^{-} progeny were isolated and expanded under FSB for five passages as in (A) and then FACS analyzed (Figure S3H). H9 hESC-derived, FSB-expanded cells in (B) were used as the GFP-negative control.

(F) Chondrogenic activity of the CD271^{hi} or CD271^{lo} progeny maintained under FSB. Cells were grown under FSB and F conditions for five passages and subjected to 2D-micromass cultures, followed by Alcian Blue staining and quantification. *p < 0.05 (n = 3 independent cultures, two masses/culture, mean ± SD).

p4–p5 (Figures 4A and 4C), in keeping with the loss of the CD271^{+} cell population (Figures 2C and S3D).

On the other hand, the (FGF2+SB431542)-expanded cells did not form a particle when subjected directly to pellet culture (no pellet, Figure 4B), suggesting that (FGF2+SB431542)-expanded cells are defective in the induction of mesenchymal condensation, a prerequisite for cartilage formation. Supporting this suggestion, 2D-micromass culture demonstrated that inclusion of SB431542 until the point of induction of chondrogenesis using TGFβ3 and BMP4 severely inhibited or delayed the formation of cartilage nodules (Figures S4A and S4B). Thus, suppression of Nodal/Activin/TGFβ signaling allows the CD271^{+}CD73^{+} cells to grow but not to initiate chondrogenesis under the action of TGFβ and BMP.

A brief treatment ("priming") with TGFβ is known to commit mouse neural crest stem cells to mesenchymal lineages (John et al., 2011). Therefore, we reasoned that stimulation with TGFβ before pellet culture might be required for efficient cartilage particle formation. When the (FGF2+SB431542)-expanded cells were passaged once into CDM containing FGF2+TGFβ3 (FT), cultured for 3 to 4 days to confluence, and then subjected to 3D-pellet culture, large translucent full-cartilage particles filled with

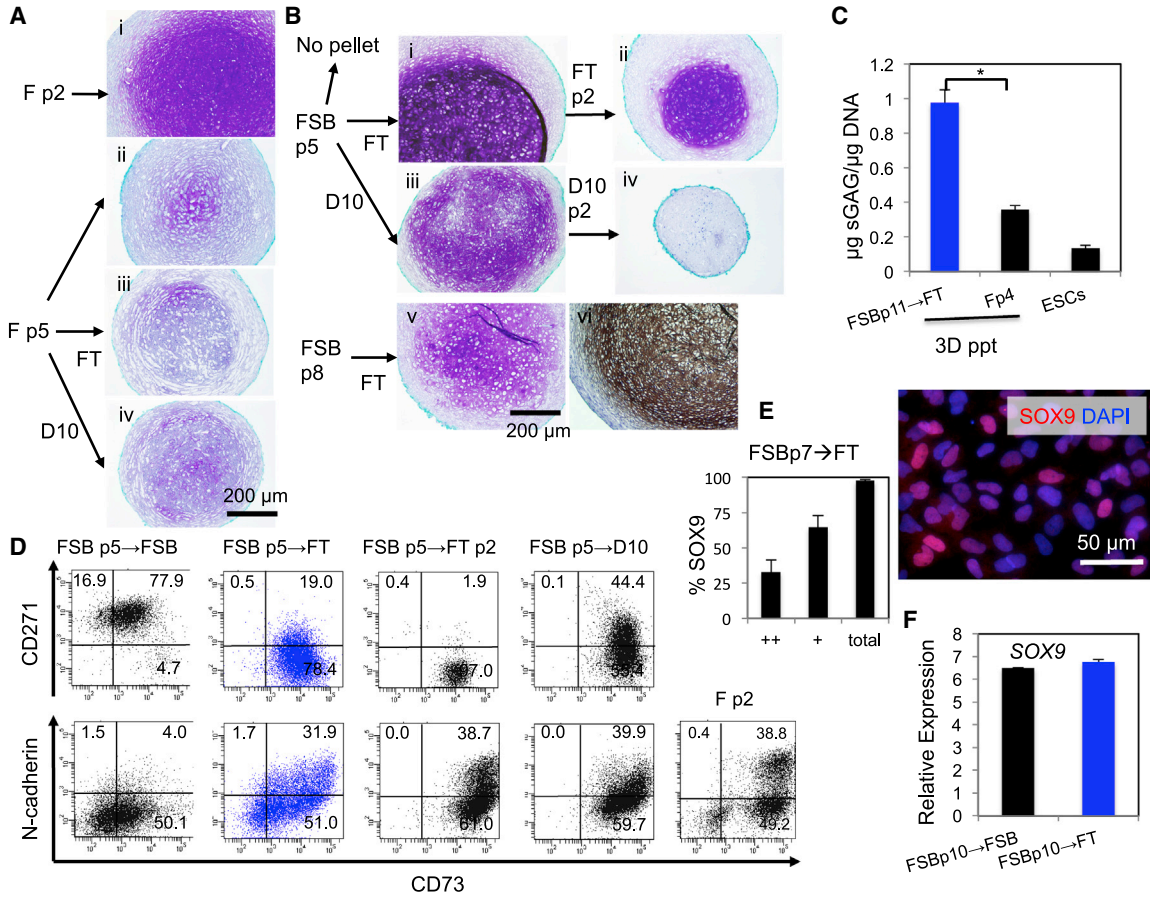

Figure 4. Pretreatment with TGFβ Facilitates Cartilage Particle Formation from the FSB-Expanded Ectomesenchymal Cells

(A and B) Cartilage particle formation from the H9 hESC-derived ectomesenchymal cells maintained under F (A) or FSB (B) by 3D-pellet culture. Toluidine Blue staining (purple) of sections of the cartilage particles, except for (Bvi), which is COL2 immunostained (brown). Some cultures were passaged once or twice (p2) to FT (CDM plus FGF2+TGFβ3) (Aiii, Bi, Bii, Bv, Bvi), or D10 (Aiv, Biii, Biv), prior to pellet culture.

(C) Capacity of sGAG production in cartilage particles. The ectomesenchymal cells cultured as indicated (→FT, passage to FT) were subjected to pellet culture and total DNA and sGAGs were quantified. Negative control: undifferentiated ESCs. *$p < 0.05$ ($n = 3$ independent cultures, one pellet/culture mean ± SD).

(D) Upregulation of N-cadherin surface expression on the FSB-expanded ectomesenchymal cells during FT treatment. The ectomesenchymal cells maintained under F (Fp2) and FSB (FSBp5) were either passaged to FSB (→FSB), FT (→FT, FTp2), or D10 (→D10) or not passaged (Fp2), and then FACS analyzed.

(E) Effect of FT treatment on SOX9 protein expression. FSB-expanded p7 ectomesenchymal cells followed by FT culture (i.e., p8) were treated and analyzed as in Figure 3D. Graph, $n = 4$ technical repeats, mean ± SD. Isotype control, Figure S4J.

(F) Real-time RT-PCR analysis for investigating the effect of FT treatment on *SOX9* gene expression ($n = 3$ technical repeats, mean ± SD).

matrices that stained metachromatically with Toluidine Blue and immunostained with the COL2 antibody were generated effectively (Figures 4Bi, 4Bv, 4Bvi, S4F, and S4H). The SB431542-dependent maintenance of chondrogenic activity during expansion culture was confirmed by the quantitative comparison of sulfated glycosaminoglycan (sGAG) levels in 24 days of pellet culture using ectomesenchymal cells maintained under FGF2+SB431542 (FSBp11→FT) and under FGF2 alone (Fp4) (Figure 4C).

When FGF2+TGFβ3 pretreatment was extended for a few more passages (FTp2), the cells maintained their particle-forming capability but gradually lost their chondrogenic potential, resulting in particles with a small cartilaginous area (Figure 4Bii). Pretreatment with D10 medium also induced pellet-forming activity in the (FGF2+SB431542)-expanded cells, which led to a full-cartilage particle (Figure 4Biii), but further maintenance in D10 completely suppressed chondrogenic activity (Figure 4Biv). Neither pretreatment was able to recover lost chondrogenic activity

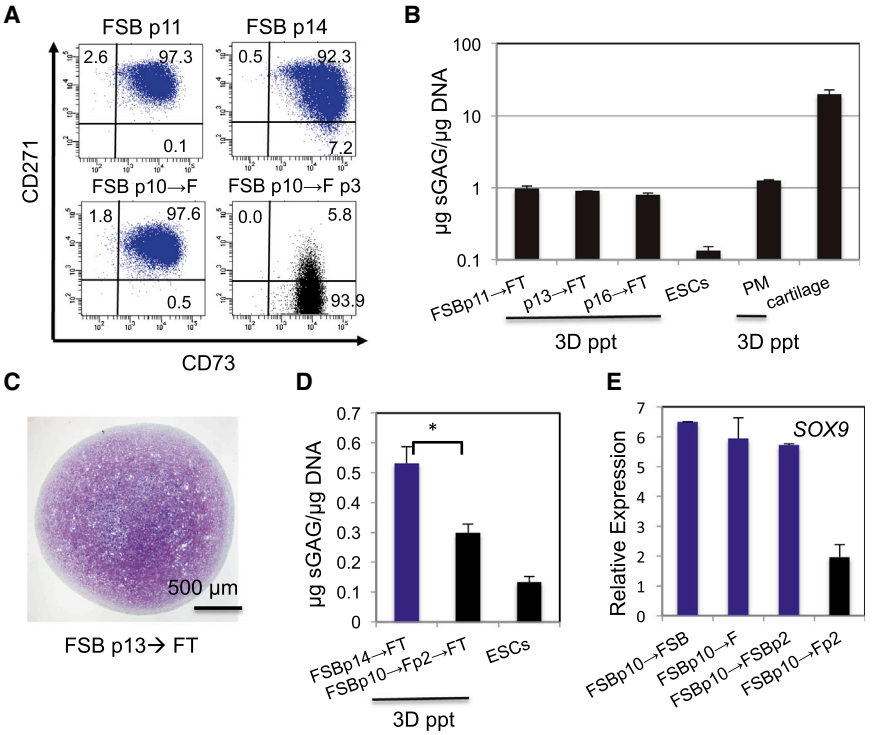

Figure 5. The Long-Term Expanded Ectomesenchymal Cells Are Still Dependent on FSB

(A) SB431542-dependent maintenance of CD271 expression. Ectomesenchymal cells maintained under FSB (p10) were either passaged one to three times to FSB again (p11, p14), or to FGF2 (→F, Fp3) and then FACS analyzed.

(B) Maintenance of sGAG production capacity. The ectomesenchymal cells maintained under FSB for 11–16 passages followed by FT treatment, and the freshly isolated chondrogenic paraxial mesoderm (PM) (Umeda et al., 2012) were subjected to pellet culture. The capacity for sGAG production is displayed as in Figure 4C. Negative control, hESCs; positive control, bovine articular cartilage (n = 3 technical repeats, mean ± SD).

(C) "Full-cartilage"-forming capacity remained in the FSB-expanded p13 ectomesenchymal cells derived from CD271^{hi}CD73^{-} H9 progeny. Toluidine Blue staining.

(D) SB431542-dependent maintenance of chondrogenic activity. The p10 ectomesenchymal cells were passaged to either FSB for four passages (FSBp14) or F for two passages (→Fp2) and then subjected to FT treatment and 3D-pellet culture. The capacity for sGAG production is displayed as in (B). *$p < 0.05$ ($n \geq 3$ independent cultures, one pellet/culture, mean ± SD).

(E) Real-time RT-PCR analysis for investigating the effect of FSB on maintaining *SOX9* expression (n = 3 technical repeats, mean ± SD).

in FGF2-expanded cells (Figures 4Aiii and 4Aiv). A brief TGFβ pretreatment thus seemed to enhance the condensing capacity but not the chondrocyte-forming ability of the expanded ectomesenchymal cells. In support of this observation, the proportion of cells expressing SOX9 protein increased only slightly from 76%–83% (Figure 3D) to 97% (Figure 4E), and the transcription levels of *SOX9* (Figure 4F), *SOX5*, and *SOX6* (data not shown) were unaltered by the 4-day FGF2+TGFβ3 treatment.

In contrast, FGF2+TGFβ3 treatment (→FT, Figure 4D) led to dramatic downregulation of the expression of CD271 in 3 to 4 days and complete loss of expression during the subsequent culture for two passages (→FTp2). A similar change was observed with D10 treatment. Since the short-term (FGF2+TGFβ3)-treated cells effectively formed cartilage particles (Figures 4Bi, 4Biii, and 4Bv), the reduction/loss of CD271 expression may be an early indicator that chondrogenic activity will be lost later.

TGFβ upregulates the production of extracellular matrix proteins and cell surface molecules such as fibronectin, N-cadherin, and N-CAM (CD56), which are involved in the initiation of precartilaginous mesenchymal condensation (Chimal-Monroy and Díaz de León, 1999). CD56 but not N-cadherin was expressed on most of the (FGF2+SB431542)-expanded ectomesenchymal cells (Figures 4D and S3E). However, treatment with FGF2+TGFβ3 or D10 resulted in the upregulation of N-cadherin. In addition, the (FGF2+SB431542)-expanded cells exposed to FGF2+TGFβ3 for two passages and the FGF2-expanded cells (Fp2) accumulated distinct N-cadherin^{lo} and N-cadherin^{+} populations. Together the results support the hypothesis that brief pretreatment with TGFβ enhances the precartilaginous condensing capacity of the ectomesenchymal cells expanded under FGF2+SB431542 conditions.

Property of the CD271^{+}CD73^{+} Cells Maintained under FGF2+SB431542 for an Extended Period

Since CD271^{+}CD73^{+} ectomesenchymal cells maintained under FGF2+SB431542 for a long time might select a rare "permanent CD271^{+} chondrogenic cell" from the original neural crest cell population, late-passage (p10) cells were subjected to medium change to CDM with FGF2 alone. All cells started losing the CD271 expression in FGF2 and nearly 95% became CD271^{-}CD73^{+} by passage 3 (Figure 5A). Those maintained in FGF2+SB431542 for four more passages were still CD271^{+}CD73^{+}, suggesting that maintenance of CD271 surface expression remained dependent on the presence of SB431542.

Furthermore, when 3D-pellet culture was performed, the (FGF2+SB431542)-expanded ectomesenchymal cells maintained their chondrogenic activity during further expansion (p11–16), as judged by the accumulation of sGAGs in the developed cartilage particles (Figure 5B), and the "full cartilage"-forming activity was preserved at least to p13 (Figure 5C). Interestingly, such chondrogenic activity was indistinguishable from that of the KDR^{-}PDGFRα^{+} chondrogenic paraxial mesodermal cells (PM) we previously reported (Umeda et al., 2012). However, even two passages without SB431542 caused the p10 cells to begin showing signs of decline in their capacity to generate similar chondrocytes in quantity and quality (→Fp2, Figures 5D and 5E). These results indicate that expansion under FGF2+SB431542 conditions does not select a permanently chondrogenic CD271^{+} cell type and that continuous suppression of the endogenous Nodal/Activin/TGFβ signaling is necessary for preventing the loss of chondrogenic activity and CD271 expression for an extended period.

The Presence of SB431542 Maintains Expression of Genes Representing "Proliferative" and "Primitive" Stages of Differentiating Neural Crest

We performed genome-wide, comparative transcriptome analyses to elucidate the molecular basis of the effect of Nodal/Activin/TGFβ signaling-suppression on the maintenance of the proliferative and chondrogenic properties of the CD271^{+}CD73^{+} ectomesenchymal cells. The CD271^{hi}CD73^{-} neural crest-like progeny of H9 hESCs were isolated and expanded under FGF2+SB431542 conditions for six to seven passages (FSB, Figure 6). In some cases, the culture condition was shifted to the FGF2 condition from p4 (FSB→F). As a control, the CD271^{hi}CD73^{-} cells were cultured from the outset under FGF2-conditions (F) for six passages.

The overall mRNA profiles of the three resultant cell populations demonstrated that (FGF2+SB431542)-expanded neural crest cells are distinct from both FGF2- and (FGF2+SB431542→FGF2)-expanded cells (Figures 6A and 6B), whereas little distinction was found between the last two. However, the possibility remained that the FGF2-cultured neural crest cells are different types of cells from (FGF2+SB431542)-expanded cells. Therefore, to investigate the effect of TGFβ suppression, further comparative analyses focused on (FGF2+SB431542)- and (FGF2+SB431542→FGF2)-cultured cells.

First, gene ontology (GO) analysis suggested that (FGF2+SB431542)-expanded cells would likely be involved in "DNA replication," "mitotic cell cycle," and "cell division" (Figure 6D), while (FGF2+SB431542→FGF2)-cultured cells seemed to have the property of differentiated cells and would likely be involved in "cell adhesion," "angiogenesis," and/or "skeletal system development." Furthermore, as for the predicted developmental potentials, (FGF2+SB431542)-expanded cells still showed relevance to "peripheral nervous system development," "melanocyte differentiation," and/or "eye development" (Figure 6D), although essential genes such as *SOX10*, *ASCL1-4*, *NEUROD1/2/4/6*, *NEUROG1-3*, *OLIG1-3*, *MITF*, and *PAX6* (Nelms and Labosky, 2010) were either not (yet) expressed or expressed at very low levels (FPKM $\leq$1; data not shown). In contrast, (FGF2+SB431542→FGF2)-cultured cells seemed to be associated more with "ossification," "odontogenesis," and "embryonic vicerocranium morphogenesis." In addition, consistent with the removal of SB431542, enhancement of "TGFβ receptor signaling" was suggested.

Comparison of genes in either cell population that showed more than a 2.5-fold difference in expression level (Figure 6C; Tables S3 and S4) supported the GO analysis in that genes preferentially expressed under FGF2+SB431542 conditions represented many, if not all, aspects of neural crest (stem) cells and primitive ectomesenchyme. Such genes included *LIN28A/B*, *TRIM71(LIN41)* and *MYCN* (Ecsedi and Grosshans, 2013; Rehfeld et al., 2015), *TWIST1/2*, *ALX1/3/4*, *SOX8/9* (Nelms and Labosky, 2010), and *NES* as well as stem cell factor receptor (*KIT*). In contrast, *TGFB3* and other TGFβ-induced genes such as *DCN* and *THBS1/2* were induced when SB431542 was removed (FSB→F). Interestingly, the FGF2+SB431542 condition supported the expression of *COL2A1*, the type II collagen gene, SOX9 regulator genes such as *MAF* (Huang et al., 2002) and *ZBTB16* (Liu et al., 2011), and *LBH* (Powder et al., 2014), while the FGF2+SB431542→FGF2 condition induced *COL1A1/1A2* and *RUNX1/2* expression, supporting their predicted "ossification" function. Consistent with FACS analyses, expression of *NGFR* (CD271), the cell surface marker gene for neural crest, was found to be supported under FGF2+SB431542 conditions, and *ANPEP* (CD13) was induced under FGF2+SB431542→FGF2. On the other hand, among genes commonly expressed in cells cultured under both conditions, the presence of *SOX4* and *SOX12* supports the likelihood that both are embryonic neural/mesenchymal progenitor cells (Bhattaram et al., 2010).

In Vivo Stability of the Cartilage Particle Developed In Vitro with the CD271^{+}CD73^{+} Cells: A Comparative Analysis

Cartilage particles generated under standard "PDGF/TGFβ/BMP" conditions (Umeda et al., 2012) with the CD271^{+}CD73^{+} ectomesenchymal cells, derived either from a mixture of the 6-day differentiated H9 hESCs or from the FACS-isolated CD271^{hi}CD73^{-} neural crest-like progeny (Figures 7C and 7D), were all mineralized after subcutaneous transplantation into immunocompromized mice for 8–12 weeks (black area with von Kossa staining),

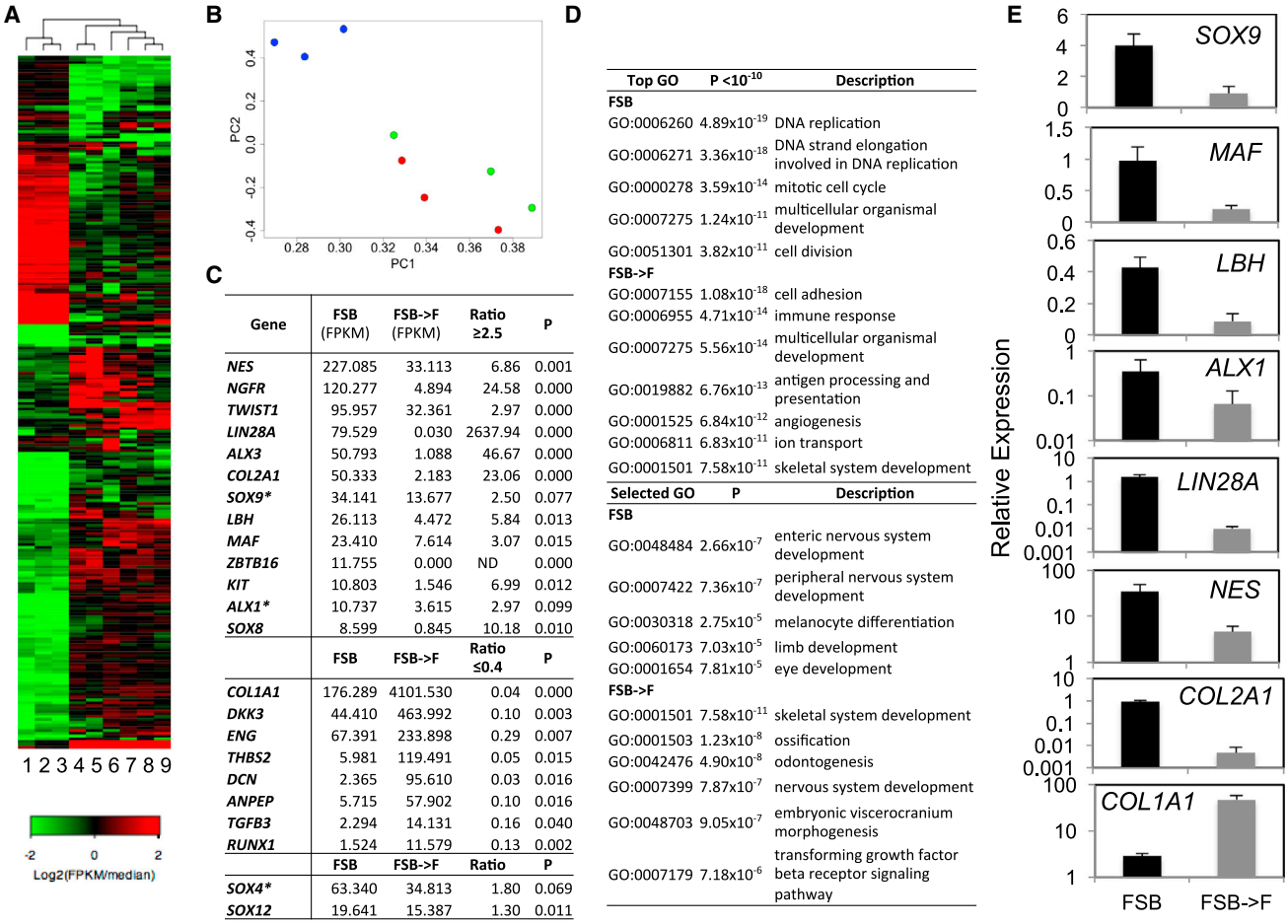

C

Gene	FSB (FPKM)	FSB->F (FPKM)	Ratio ≥2.5	P
NES	227.085	33.113	6.86	0.001
NGFR	120.277	4.894	24.58	0.000
TWIST1	95.957	32.361	2.97	0.000
LIN28A	79.529	0.030	2637.94	0.000
ALX3	50.793	1.088	46.67	0.000
COL2A1	50.333	2.183	23.06	0.000
*SOX9**	34.141	13.677	2.50	0.077
LBH	26.113	4.472	5.84	0.013
MAF	23.410	7.614	3.07	0.015
ZBTB16	11.755	0.000	ND	0.000
KIT	10.803	1.546	6.99	0.012
*ALX1**	10.737	3.615	2.97	0.099
SOX8	8.599	0.845	10.18	0.010
	FSB	**FSB->F**	**Ratio ≤0.4**	**P**
COL1A1	176.289	4101.530	0.04	0.000
DKK3	44.410	463.992	0.10	0.003
ENG	67.391	233.898	0.29	0.007
THBS2	5.981	119.491	0.05	0.015
DCN	2.365	95.610	0.03	0.016
ANPEP	5.715	57.902	0.10	0.016
TGFB3	2.294	14.131	0.16	0.040
RUNX1	1.524	11.579	0.13	0.002
	FSB	**FSB->F**	**Ratio**	**P**
*SOX4**	63.340	34.813	1.80	0.069
SOX12	19.641	15.387	1.30	0.011

D

Top GO	P <10^{-10}	Description
FSB		
GO:0006260	4.89×10^{-19}	DNA replication
GO:0006271	3.36×10^{-18}	DNA strand elongation involved in DNA replication
GO:0000278	3.59×10^{-14}	mitotic cell cycle
GO:0007275	1.24×10^{-11}	multicellular organismal development
GO:0051301	3.82×10^{-11}	cell division
FSB->F		
GO:0007155	1.08×10^{-18}	cell adhesion
GO:0006955	4.71×10^{-14}	immune response
GO:0007275	5.56×10^{-14}	multicellular organismal development
GO:0019882	6.76×10^{-13}	antigen processing and presentation
GO:0001525	6.84×10^{-12}	angiogenesis
GO:0006811	6.83×10^{-11}	ion transport
GO:0001501	7.58×10^{-11}	skeletal system development

Selected GO	P	Description
FSB		
GO:0048484	2.66×10^{-7}	enteric nervous system development
GO:0007422	7.36×10^{-7}	peripheral nervous system development
GO:0030318	2.75×10^{-5}	melanocyte differentiation
GO:0060173	7.03×10^{-5}	limb development
GO:0001654	7.81×10^{-5}	eye development
FSB->F		
GO:0001501	7.58×10^{-11}	skeletal system development
GO:0001503	1.23×10^{-8}	ossification
GO:0042476	4.90×10^{-8}	odontogenesis
GO:0007399	7.87×10^{-7}	nervous system development
GO:0048703	9.05×10^{-7}	embryonic viscerocranium morphogenesis
GO:0007179	7.18×10^{-6}	transforming growth factor beta receptor signaling pathway

Figure 6. Comparative Transcriptome Analysis of Ectomesenchymal Cells Using the RNA-seq Technology

(A) Heat map of the top 250 genes, which are differentially expressed among the three groups. Lanes 1–3: "FSB"; lanes 4, 5, 8: "F"; lanes 6, 7, 9: "FSB → F."

(B) Principal component analysis of the expression pattern of protein-coding genes among the three groups. Blue, "FSB"; red, "F"; green, "FSB → F."

(C) Selected list of culture condition-specific genes and common genes. Genes that gave a $p < 0.05$ were picked from Tables S3 and S4 except for few with * that gave slightly more variations ($0.05 < p < 0.1$). ND, not determined.

(D) GO analysis. Selected GO categories from Table S1 (upper) and a selected list of development-related GO terms from Table S2 (lower).

(E) RT-PCR confirmation of the relative gene expression levels predicted by the FPKM values (n = 3 independent cultures, mean ± SD).

implying the capacity of the $CD271^+CD73^+$ cell to induce endochondral ossification. Consistently, the detection of *RUNX2* transcript (2D-micromass culture, Figure 7E) and *COL10A1* transcript (3D-pellet culture, Figure 7F) during chondrogenesis suggested that the ectomesenchymal cell-derived chondrocytes matured into hypertrophic chondrocytes.

Such a property of the ectomesenchymal cells might reflect a more general property of hPSC-derived chondrogenic cells. Therefore, we also examined the cartilage particles produced by the hPSC-derived $KDR^-PDGFR\alpha^+$ chondrogenic paraxial mesodermal progeny (Umeda et al., 2012). First, we significantly improved the yield of $KDR^-PDGFR\alpha^+$ progeny expressing higher levels of *MEOX1*, *TCF15*, as well as *UNCX* (Figure S5) by replacing BIO with CHIR99021 and inhibiting FGF signaling with PD173074 at a later stage of differentiation. Next, cartilage particles were generated and transplanted subcutaneously. The transplanted particles were mineralized at the periphery, but four of six particles stably maintained internal unmineralized cartilaginous areas even after 12 weeks (Figure 7A). In some case, the whole cartilaginous particles remained unmineralized (Figure 7B). These results indicate that the strong tendency of terminal

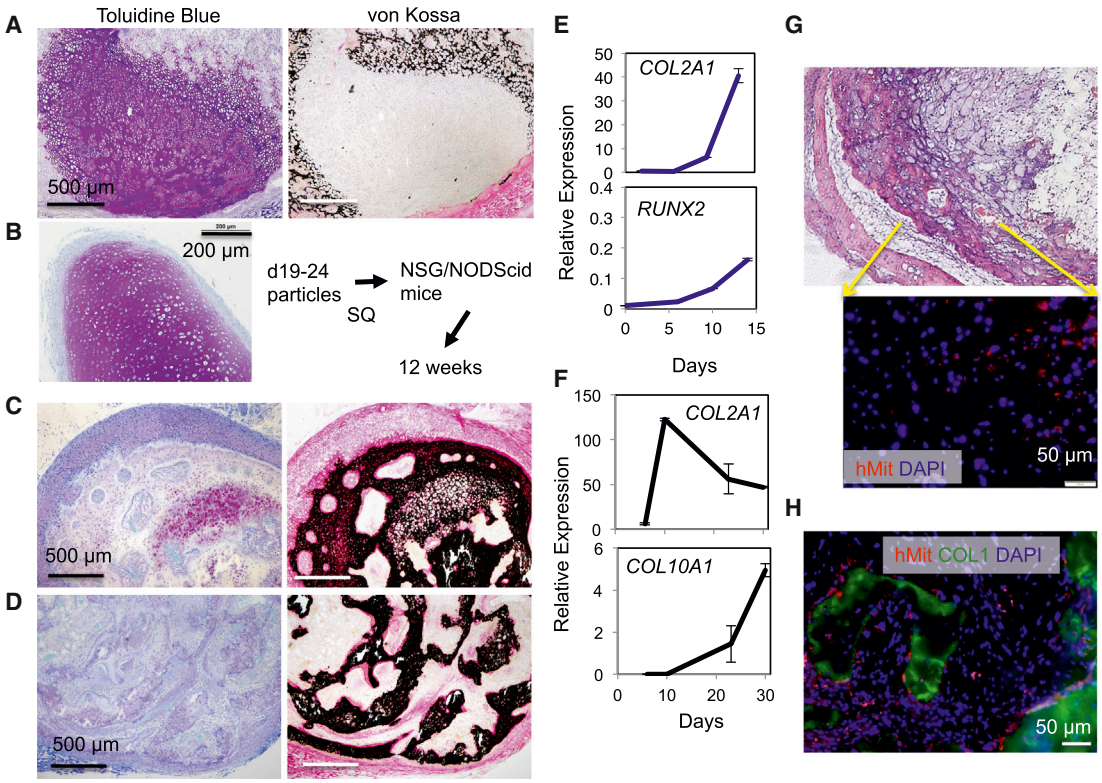

Figure 7. In Vivo Stability of Cartilage Particles Developed with the CD271$^+$CD73$^+$ Ectomesenchymal Cells

(A–D) In vivo maturation of cartilage particles developed with the FSB-expanded CD271$^+$CD73$^+$ ectomesenchymal cells (C and D), generated from H9 hESC-derived CD271^{hi}CD73$^-$ neural crest-like progeny in comparison with those developed with the freshly isolated KDR$^-$PDGFRα^+ paraxial mesoderm, derived from H9 hESCs under the CHIR99021-based 4i+P conditions (A) and from HES3 hESCs under the BIO-based 2i condition (B) (Umeda et al., 2012). Cartilage particles were transplanted into NSG mice (A, C, and D) and NODScid mice (B) subcutaneously for 12 weeks, recovered, fixed, sectioned, and stained with Toluidine Blue (cartilaginous area is in purple) and von Kossa (bony area is in black).

(E and F) Cartilage gene expression during chondrogenesis cultures. The FSB-expanded p7 cells were subjected to 2D-micromass culture (E) or 3D-pellet culture (F) and then real-time RT-PCR (n = 3 technical repeats, mean ± SD).

(G and H) Immunostaining with anti-human mitochondria (hMit) antibody. Sections of a bony particle made in (C) and (D) were stained with H&E (G) or stained with hMit antibody (pink, G and H) and anti-type I collagen (COL1) antibody (green, H), followed by counterstaining with DAPI (blue). Negative controls, Figures S4K and S4L.

maturation in vivo is not a general property of the hPSC-derived chondrogenic progeny. The neural crest-derived ectomesenchymal cells may innately possess such a property or may have been primed for it during expansion.

Endochondral ossification would replace the transplanted cartilage (consisting of human chondrocytes) with bone tissue made by osteoblasts and osteocytes of murine origin. We therefore addressed the question of whether the donor human chondrocytes completely disappeared from the bony particles generated in 12 weeks. As expected, immunohistochemical analyses revealed that the large hypertrophic chondrocytes showed human-specific signals (Figure 7G). Interestingly, human cells were also detected in a marrow-like space and around the COL1-positive bone pieces (Figure 7H), suggesting that the transplanted cartilage particles may contain cells with osteoblastic/osteocytic potential.

DISCUSSION

We have established a novel serum-free culture method for generating and expanding CD271$^+$CD73$^+$SOX9$^+$ chondrogenic ectomesenchymal cells from hPSC-derived, CD271^{hi}CD73$^-$ neural crest-like progeny. The differentiation pathways from hPSCs to chondrocytes via chondrogenic ectomesenchymal cells postulated from this study are summarized in the Graphical Abstract. Under optimal conditions, the generation of neural crest-like progeny

from hPSCs in CDM was achieved more quickly than previously reported, and the resultant ectomesenchymal cells displayed long-term chondrogenic activity.

Quantitative data on the efficiency of genesis of SOX9-expressing chondroprogenitors from hESCs were first shown by Oldershaw et al. (2010). Under their conditions in which hESC differentiation is directed initially to mesoderm then toward chondrocytes, approximately 8.5 chondroprogenitors of 75%–97% $SOX9^+$ are produced per hESC by day 14 of differentiation. In contrast, while only about 0.6 $CD271^{hi}CD73^-$ neural crest-like progeny were generated per hPSC by day 6 of differentiation in CDM plus SB431542 (data not shown), our method for neural crest-like cell culture in CDM in the presence of FGF2+SB431542 led to 19 to 38 $CD271^+CD73^+$ chondroprogenitors per hPSC by day 14 (Figure S3A). Approximately 76%–85% of these cells continued to express SOX9 protein on days 27–33 (p8–p10), a proportion that increased slightly to about 97% after 3 days of treatment with FGF2+TGFβ3. Further expansion yielded approximately 1×10^7 chondrogenic ectomesenchymal cells per hPSC by day 51 (p16, 24 population doublings). Thus, the method described here allows human chondrogenic cells to expand for an extended period without the loss of purity and chondrogenic activity, resulting in a much larger yield of chondroprogenitor cells (although not homogenous) from hPSCs than previously attained.

The effect of SB431542 on expansion of endothelial progenitors derived from mouse and human ESCs has also been reported (James et al., 2010; Watabe et al., 2003). A lack of Nodal/Activin/TGFβ signaling may generally promote proliferation and prevent terminal differentiation of embryonic stem/progenitor cells. In this respect, the ways in which FGF2+SB431542 helps to maintain SOX9 and CD271 while suppressing N-cadherin expression during expansion of the chondrogenic $CD271^+CD73^+$ cells and in which $CD271^{hi}CD73^-$ neural crest-like cells are directed to give rise to such cells are interesting topics for future study. In this respect, comparative transcriptome analysis has revealed that the $CD271^+CD73^+$ cells accumulated under FGF2+SB431542 conditions possess a similar mRNA profile to primitive neural crest/ectomesenchymal cells, although they lacked *SOX10* expression, which is critical for neural and melanocytic lineage commitment. Thus, suppression of Nodal/Activin/TGFβ signaling does not seem to freeze the developmental stage of the hPSC-derived neural crest during expansion. Such suppression may instead simply support the high proliferative potential of the cells as well as the expression of SOX9 (and *COL2A1*), and thereby maintain chondrogenic activity. *SOX9* expression initiated at the specification and premigratory stages is transient in trunk neural crest but persists in cranial neural crest (Cheung and Briscoe, 2003; Cheung et al., 2005; McKeown et al., 2005). The chondrogenic $CD271^+CD73^+$ ectomesenchymal cells that maintain *SOX9* transcription and translation ($SOX9\text{-}GFP^{+/lo}$) may therefore represent proliferating cranial neural crest, with a slight commitment to non-neural lineages.

Genesis of MSC-like cells from hESCs directly or via neuroectoderm specification has been demonstrated (Chambers et al., 2009; Mahmood et al., 2010). As shown in Figure S4D, the colonogenic (CFU-F) activity, representing self-renewal activity of MSCs, emerged as early as p2 of the expansion culture under FGF2 alone (i.e., in $CD271^-$ CD73 cells) or FGF2+SB431542 (i.e., in $CD271^+CD73^+$ cells). However, we were unable to demonstrate significant adipogenic or osteogenic activity in either cell type (data not shown), although the GO analysis predicted osteogenic activity in cells generated under FGF2 (data not shown) and FGF2+SB431542 → FGF2 conditions. This discrepancy may be due to some degree of heterogeneity in the cell types generated under these conditions or to the assay method employed, which is widely used for MSCs (Pittenger et al., 1999), but is less well validated for mesenchymal cells derived from human neural crest. Furthermore, the FGF2+SB431542 conditions applied to the expansion culture of mouse bone marrow MSCs resulted in inhibition of proliferation and promotion of adipocytic differentiation (data not shown). The $CD271^+CD73^+$ ectomesenchymal cells are therefore very likely not to be MSCs, although the possibility that they are derived from an MSC-like precursor has not been excluded.

Thus, hPSC-derived chondrogenic ectomesenchymal cells are amenable to large-scale production in CDM without loss of activity. Although some hESC-derived neural crest stem cells are known to self-renew in culture for an extended period, during which they maintain the capacity to produce multipotential MSC-like activity (Menendez et al., 2011), no previous reports have described a method as simple and effective as ours for generating large quantities of (osteo)chondrogenically committed mesenchymal cells under clinically applicable, defined conditions. Therefore, the chondrogenic ectomesenchymal cells produced by the culture technology described are set to become a competitive alternative to adult MSCs, especially for craniofacial regenerative therapy. Moreover, taking advantage of high yields of chondroprogenitor cells, we have successfully modeled neonatal-onset multisystem inflammatory disease by applying our method to patient-derived iPSCs (Yokoyama et al., 2015).

EXPERIMENTAL PROCEDURES

Cells

H9 (WA09), HES3 (ES03), MIXL1-GFP hESCs, and the human fibroblast-derived iPSC line, BJ5, were maintained on feeder cells as described (Umeda et al., 2012). The SOX9-GFP hiPSC

(CY2-SOX9-2A-ZsGreen-2A-Puro) line from NIH was maintained feeder free in E8 medium.

Neural Crest Cell Differentiation from hPSCs

For generating neural crest-like progeny, H9 hESCs and BJ5 hiPSCs were transferred to gelatin-coated dishes and cultured feeder free in the differentiation medium: CDM supplemented with SB431542. The SOX9-GFP hiPSCs were directly induced to differentiate by changing the medium to differentiation medium.

Paraxial Mesoderm Generation from hESCs

The hPSCs were differentiated as described (Umeda et al., 2012) ("2i" condition) or using improvements involving CHIR99021, Noggin, PD173074, and PDGF with or without SB431542 ("3i+P" or "4i+P," Figure S5).

Flow Cytometry

FACS analysis and cell sorting were performed as described (Umeda et al., 2012). Intracellular staining for FACS analysis using mouse anti-PAX3 monoclonal antibody was performed according to the manufacturer's recommendations.

Ectomesenchymal Cell Genesis and Expansion

The differentiated hPSCs before and after sorting for $CD271^{hi}CD73^{-}$ were plated onto fibronectin-coated dishes and cultured in CDM supplemented with FGF2 and/or SB431542 (or other small molecules) or in the serum-containing D10 medium.

Immunofluorescence Detection of SOX9

The $CD271^{hi}CD73^{-}$ neural crest-like progeny were cultured in an eight-well chamber slide for 3 days in CDM containing either FGF2+SB431542 or FGF2+TGFβ3 and immunostained with the anti-hSOX9 polyclonal antibody.

Chondrogenesis Assays

2D-micromass culture and 3D-pellet culture were performed and analyzed as described (Nakayama et al., 2003; Tanaka et al., 2009; Umeda et al., 2012).

Quantification of Sulfated Glycosaminoglycans

DNAs and sulfated glycosaminoglycans (sGAGs) from micromasses and cartilage particles were isolated, quantified, and analyzed as described (Zhao et al., 2014).

Subcutaneous Transplantation and Immunohistological Analysis

Cartilaginous particles were transplanted under the dorsal skin of NODScid or NODScid $Il2rg^{-/-}$ (NSG) mice for 8–12 weeks and analyzed as described (Zhao et al., 2014). To detect remaining human cells, the fixed particles were first decalcified and then paraffin embedded, sectioned, and stained with the mouse antihuman mitochondria monoclonal antibody.

Gene-Expression Profiling

Total RNAs were isolated and reverse transcribed (RT), and real-time PCR was performed using the Taqman Gene Expression Assay. The results were displayed as described (Zhao et al., 2014). RNA sequencing was performed on an Illumina HiSeq 1500. Sequenced reads were deposited to Gene Expression Omnibus (GSE64752) and mapped against the human reference genome (GRCh37). Expression levels were calculated as fragments per kilobase of exon per million mapped fragments (FPKMs) (Tables S1, S2, S3, and S4).

SUPPLEMENTAL INFORMATION

Supplemental Information includes Supplemental Experimental Procedures, six figures, and four tables and can be found with this article online at http://dx.doi.org/10.1016/j.stemcr.2015.02.012.

ACKNOWLEDGMENTS

We acknowledge A. Crane and W. Liao for providing BJ5 hiPSCs; D. Havilland and A. Hazen for cell sorting; N. Brouard for subcutaneous transplantation; J. Lee, D. Mora Ortiz, and S. Trilok for real-time PCR; S. Amra and M. Starbuck for histological analyses; Z. Mao and N. Brouard for immunofluorescence analyses; P. Simmons for STRO1 antibody; and M. Rao at NIH Center for Regenerative Medicine for CY2-SOX9-2A-ZsGreen-2A-Puro hiPSCs. This work was supported by Brown Foundation Institute of Molecular Medicine, UTHealth (Startup Fund, N.N.), by Rolanette and Berdon Lawrence Bone Disease Program of Texas Research Award (N.N.), and by the Arthritis Foundation (N.N.).

Received: December 12, 2013
Revised: February 18, 2015
Accepted: February 19, 2015
Published: March 26, 2015

REFERENCES

Abzhanov, A., Tzahor, E., Lassar, A.B., and Tabin, C.J. (2003). Dissimilar regulation of cell differentiation in mesencephalic (cranial) and sacral (trunk) neural crest cells in vitro. Development *130*, 4567–4579.

Bakre, M.M., Hoi, A., Mong, J.C., Koh, Y.Y., Wong, K.Y., and Stanton, L.W. (2007). Generation of multipotential mesendodermal progenitors from mouse embryonic stem cells via sustained Wnt pathway activation. J. Biol. Chem. *282*, 31703–31712.

Betters, E., Liu, Y., Kjaeldgaard, A., Sundström, E., and García-Castro, M.I. (2010). Analysis of early human neural crest development. Dev. Biol. *344*, 578–592.

Bhattaram, P., Penzo-Méndez, A., Sock, E., Colmenares, C., Kaneko, K.J., Vassilev, A., Depamphilis, M.L., Wegner, M., and Lefebvre, V. (2010). Organogenesis relies on SoxC transcription factors for the survival of neural and mesenchymal progenitors. Nat. Commun. *1*, 9.

Chambers, S.M., Fasano, C.A., Papapetrou, E.P., Tomishima, M., Sadelain, M., and Studer, L. (2009). Highly efficient neural conversion of human ES and iPS cells by dual inhibition of SMAD signaling. Nat. Biotechnol. *27*, 275–280.

Cheung, M., and Briscoe, J. (2003). Neural crest development is regulated by the transcription factor Sox9. Development *130*, 5681–5693.

Cheung, M., Chaboissier, M.C., Mynett, A., Hirst, E., Schedl, A., and Briscoe, J. (2005). The transcriptional control of trunk neural crest induction, survival, and delamination. Dev. Cell *8*, 179–192.

Chimal-Monroy, J., and Díaz de León, L. (1999). Expression of N-cadherin, N-CAM, fibronectin and tenascin is stimulated by TGF-beta1, beta2, beta3 and beta5 during the formation of precartilage condensations. Int. J. Dev. Biol. *43*, 59–67.

Craft, A.M., Ahmed, N., Rockel, J.S., Baht, G.S., Alman, B.A., Kandel, R.A., Grigoriadis, A.E., and Keller, G.M. (2013). Specification of chondrocytes and cartilage tissues from embryonic stem cells. Development *140*, 2597–2610.

Davis, R.P., Ng, E.S., Costa, M., Mossman, A.K., Sourris, K., Elefanty, A.G., and Stanley, E.G. (2008). Targeting a GFP reporter gene to the MIXL1 locus of human embryonic stem cells identifies human primitive streak-like cells and enables isolation of primitive hematopoietic precursors. Blood *111*, 1876–1884.

Diekman, B.O., Christoforou, N., Willard, V.P., Sun, H., Sanchez-Adams, J., Leong, K.W., and Guilak, F. (2012). Cartilage tissue engineering using differentiated and purified induced pluripotent stem cells. Proc. Natl. Acad. Sci. USA *109*, 19172–19177.

Ecsedi, M., and Grosshans, H. (2013). LIN-41/TRIM71: emancipation of a miRNA target. Genes Dev. *27*, 581–589.

Huang, W., Lu, N., Eberspaecher, H., and De Crombrugghe, B. (2002). A new long form of c-Maf cooperates with Sox9 to activate the type II collagen gene. J. Biol. Chem. *277*, 50668–50675.

Hwang, N.S., Varghese, S., Zhang, Z., and Elisseeff, J. (2006). Chondrogenic differentiation of human embryonic stem cell-derived cells in arginine-glycine-aspartate-modified hydrogels. Tissue Eng. *12*, 2695–2706.

James, D., Nam, H.S., Seandel, M., Nolan, D., Janovitz, T., Tomishima, M., Studer, L., Lee, G., Lyden, D., Benezra, R., et al. (2010). Expansion and maintenance of human embryonic stem cell-derived endothelial cells by TGFbeta inhibition is Id1 dependent. Nat. Biotechnol. *28*, 161–166.

John, N., Cinelli, P., Wegner, M., and Sommer, L. (2011). Transforming growth factor β-mediated Sox10 suppression controls mesenchymal progenitor generation in neural crest stem cells. Stem Cells *29*, 689–699.

Koelling, S., Kruegel, J., Irmer, M., Path, J.R., Sadowski, B., Miro, X., and Miosge, N. (2009). Migratory chondrogenic progenitor cells from repair tissue during the later stages of human osteoarthritis. Cell Stem Cell *4*, 324–335.

Le Douarin, N.M., and Creuzet, S.E. (2009). Craniofacial patterning. In The Skeletal System, O. Pourquié, ed. (Cold Spring Harbor, NY: Cold Spring Harbor Laboratory Press), pp. 117–145.

Lee, G., Kim, H., Elkabetz, Y., Al Shamy, G., Panagiotakos, G., Barberi, T., Tabar, V., and Studer, L. (2007). Isolation and directed differentiation of neural crest stem cells derived from human embryonic stem cells. Nat. Biotechnol. *25*, 1468–1475.

Lee, G., Chambers, S.M., Tomishima, M.J., and Studer, L. (2010). Derivation of neural crest cells from human pluripotent stem cells. Nat. Protoc. *5*, 688–701.

Liu, T.M., Guo, X.M., Tan, H.S., Hui, J.H., Lim, B., and Lee, E.H. (2011). Zinc-finger protein 145, acting as an upstream regulator of SOX9, improves the differentiation potential of human mesenchymal stem cells for cartilage regeneration and repair. Arthritis Rheum. *63*, 2711–2720.

Mahmood, A., Harkness, L., Schrøder, H.D., Abdallah, B.M., and Kassem, M. (2010). Enhanced differentiation of human embryonic stem cells to mesenchymal progenitors by inhibition of TGF-beta/activin/nodal signaling using SB-431542. J. Bone Miner. Res. *25*, 1216–1233.

McKeown, S.J., Lee, V.M., Bronner-Fraser, M., Newgreen, D.F., and Farlie, P.G. (2005). Sox10 overexpression induces neural crest-like cells from all dorsoventral levels of the neural tube but inhibits differentiation. Dev. Dyn. *233*, 430–444.

Menendez, L., Yatskievych, T.A., Antin, P.B., and Dalton, S. (2011). Wnt signaling and a Smad pathway blockade direct the differentiation of human pluripotent stem cells to multipotent neural crest cells. Proc. Natl. Acad. Sci. USA *108*, 19240–19245.

Milet, C., and Monsoro-Burq, A.H. (2012). Neural crest induction at the neural plate border in vertebrates. Dev. Biol. *366*, 22–33.

Morrison-Graham, K., Schatteman, G.C., Bork, T., Bowen-Pope, D.F., and Weston, J.A. (1992). A PDGF receptor mutation in the mouse (Patch) perturbs the development of a non-neuronal subset of neural crest-derived cells. Development *115*, 133–142.

Nakayama, N., and Umeda, K. (2011). From pluripotent stem cells to lineage-specific chondrocytes: essential signalling and cellular intermediates. In Embryonic Stem Cells: The Hormonal Regulation of Pluripotency and Embryogenesis, C. Atwood, ed. (Wien: INTECH), pp. 621–648.

Nakayama, N., Duryea, D., Manoukian, R., Chow, G., and Han, C.Y. (2003). Macroscopic cartilage formation with embryonic stem-cell-derived mesodermal progenitor cells. J. Cell Sci. *116*, 2015–2028.

Nelms, B.L., and Labosky, P.A. (2010). Transcriptional control of neural crest development, *Volume 1* (Morgan & Claypool Life Sciences).

Nishikawa, S., Jakt, L.M., and Era, T. (2007). Embryonic stem-cell culture as a tool for developmental cell biology. Nat. Rev. Mol. Cell Biol. *8*, 502–507.

Oldershaw, R.A., Baxter, M.A., Lowe, E.T., Bates, N., Grady, L.M., Soncin, F., Brison, D.R., Hardingham, T.E., and Kimber, S.J. (2010). Directed differentiation of human embryonic stem cells toward chondrocytes. Nat. Biotechnol. *28*, 1187–1194.

Olivier, E.N., Rybicki, A.C., and Bouhassira, E.E. (2006). Differentiation of human embryonic stem cells into bipotent mesenchymal stem cells. Stem Cells *24*, 1914–1922.

Pittenger, M.F., Mackay, A.M., Beck, S.C., Jaiswal, R.K., Douglas, R., Mosca, J.D., Moorman, M.A., Simonetti, D.W., Craig, S., and Marshak, D.R. (1999). Multilineage potential of adult human mesenchymal stem cells. Science *284*, 143–147.

Powder, K.E., Cousin, H., McLinden, G.P., and Craig Albertson, R. (2014). A nonsynonymous mutation in the transcriptional regulator lbh is associated with cichlid craniofacial adaptation and neural crest cell development. Mol. Biol. Evol. *31*, 3113–3124.

Rehfeld, F., Rohde, A.M., Nguyen, D.T., and Wulczyn, F.G. (2015). Lin28 and let-7: ancient milestones on the road from pluripotency to neurogenesis. Cell Tissue Res. *359*, 145–160.

Santagati, F., and Rijli, F.M. (2003). Cranial neural crest and the building of the vertebrate head. Nat. Rev. Neurosci. *4*, 806–818.

Smith, J.R., Vallier, L., Lupo, G., Alexander, M., Harris, W.A., and Pedersen, R.A. (2008). Inhibition of Activin/Nodal signaling promotes specification of human embryonic stem cells into neuroectoderm. Dev. Biol. *313*, 107–117.

Somoza, R.A., Welter, J.F., Correa, D., and Caplan, A.I. (2014). Chondrogenic differentiation of mesenchymal stem cells: challenges and unfulfilled expectations. Tissue Eng. Part B Rev. *20*, 596–608.

Stemple, D.L., and Anderson, D.J. (1992). Isolation of a stem cell for neurons and glia from the mammalian neural crest. Cell *71*, 973–985.

Tanaka, M., Jokubaitis, V., Wood, C., Wang, Y., Brouard, N., Pera, M., Hearn, M., Simmons, P., and Nakayama, N. (2009). BMP inhibition stimulates WNT-dependent generation of chondrogenic mesoderm from embryonic stem cells. Stem Cell Res. (Amst.) *3*, 126–141.

Toh, W.S., Guo, X.M., Choo, A.B., Lu, K., Lee, E.H., and Cao, T. (2009). Differentiation and enrichment of expandable chondrogenic cells from human embryonic stem cells in vitro. J. Cell. Mol. Med. *13*, 3570–3590.

Umeda, K., Zhao, J., Simmons, P., Stanley, E., Elefanty, A., and Nakayama, N. (2012). Human chondrogenic paraxial mesoderm, directed specification and prospective isolation from pluripotent stem cells. Sci. Rep. *2*, 455.

Wang, Y., and Nakayama, N. (2009). WNT and BMP signaling are both required for hematopoietic cell development from human ES cells. Stem Cell Res. (Amst.) *3*, 113–125.

Watabe, T., Nishihara, A., Mishima, K., Yamashita, J., Shimizu, K., Miyazawa, K., Nishikawa, S., and Miyazono, K. (2003). TGF-beta receptor kinase inhibitor enhances growth and integrity of embryonic stem cell-derived endothelial cells. J. Cell Biol. *163*, 1303–1311.

Weston, J.A., Yoshida, H., Robinson, V., Nishikawa, S., Fraser, S.T., and Nishikawa, S. (2004). Neural crest and the origin of ectomesenchyme: neural fold heterogeneity suggests an alternative hypothesis. Dev. Dyn. *229*, 118–130.

Yokoyama, K., Ikeya, M., Umeda, K., Oda, H., Nodomi, S., Nasu, A., Matsumoto, Y., Izawa, K., Horigome, K., Kusaka, T., et al. (2015). Enhanced chondrogenesis of induced pluripotent stem cells from patients with neonatal-onset multisystem inflammatory disease occurs via the caspase 1-independent cAMP/protein kinase A/CREB pathway. Arthritis Rheumatol. *67*, 302–314.

Zhao, J., Li, S., Trilok, S., Tanaka, M., Jokubaitis-Jameson, V., Wang, B., Niwa, H., and Nakayama, N. (2014). Small molecule-directed specification of sclerotome-like chondroprogenitors and induction of a somitic chondrogenesis program from embryonic stem cells. Development *141*, 3848–3858.